Weierstraß-Institut
für Angewandte Analysis und Stochastik
Leibniz-Institut im Forschungsverbund Berlin e. V.

Preprint ISSN 0946 – 8633

Dynamical regimes of multi-stripe laser array with external off-axis feedback

Alexander Pimenov[1], Vasile Z. Tronciu[2], Uwe Bandelow[1], Andrei G. Vladimirov[1]

submitted: September 14, 2012

[1] Weierstrass Institute
Mohrenstr. 39
10117 Berlin
Germany
E-Mail: aleksandr.pimenov@wias-berlin.de
uwe.bandelow@wias-berlin.de
andrei.vladimirov@wias-berlin.de

[2] Technical University of Moldova
bd. Stefan cel Mare 168
Chisinau 2004
Republic of Moldova

No. 1731
Berlin 2012

2010 *Mathematics Subject Classification.* 78A60, 37M05, 78A45, 34K60.

2008 *Physics and Astronomy Classification Scheme.* 42.55.Px, 42.60.Mi, 42.60.Da, 42.55.Sf.

Key words and phrases. Broad-area semiconductor lasers, multi-stripe laser array, off-axis feedback, delay differential equations, bifurcation analysis.

The authors thank Gregory Kozyreff for helpful discussions. The authors acknowledge the support of SFB 787 of the DFG under Grant B5. V.T. acknowledges the support from Technical University of Moldova project 106 b/s and from CIM - Returning Experts Programme. A.G.V. acknowledges the support of the EU FP7 Initial Training Network PROPHET (Grant No. 264687), E.T.S. Walton Visitors Award of the SFI, and the program Research and Pedagogical Cadre for Innovative Russia (Grant No. 2011-1.5-503-002-038).

Edited by
Weierstraß-Institut für Angewandte Analysis und Stochastik (WIAS)
Leibniz-Institut im Forschungsverbund Berlin e. V.
Mohrenstraße 39
10117 Berlin
Germany

Fax: +49 30 20372-303
E-Mail: preprint@wias-berlin.de
World Wide Web: http://www.wias-berlin.de/

Abstract

We study theoretically the dynamics of a multistripe laser array with an external cavity formed by either a single or two off-axis feedback mirrors, which allow to select a single lateral mode with transversely modulated intensity distribution. We derive and analyze a reduced model of such an array based on a set of delay differential equations taking into account transverse carrier grating in the semiconductor medium. With the help of the bifurcation analysis of the reduced model we show the existence of single and multimode instabilities leading to periodic and irregular pulsations of the output intensity. In particular, we observe a multimode instability leading to a periodic regime with anti-phase oscillating intensities of the two counter-propagating waves in the external cavity. This is in agreement with the result obtained earlier with the help of a 2+1 dimensional traveling wave model.

1 Introduction

During the last decades high power broad area laser diodes attracted much attention due to their applications in different areas, such as medicine, spectroscopy, and material processing. These lasers reach electro-optical efficiencies of more than 70% [13] and feature small physical sizes combined with high reliability. Moreover, these devices can exhibit output powers of more than 20 W as single emitters [19] and several hundred Watts when they are combined in laser bars [17]. However, because of transverse instabilities arising at sufficiently high pump levels, broad area lasers usually demonstrate poor beam quality characterized by large far-field divergence. Furthermore, in the absence of spectral filtering they usually operate in unwanted dynamical periodic or chaotic states. Several approaches have been developed to improve the beam quality and increase the brightness of high power broad area laser diodes. Promising designs are distributed-feedback tapered master oscillator power amplifiers [21, 28] or DBR tapered lasers [5, 6, 8]. They consist of a narrow ridge waveguide for lateral mode filtering and a tapered amplifier integrated on a single chip. Another method to improve the output beam characteristics is based on the use of multi-stripe laser arrays [2]. When all N stripes in the array are synchronized in-phase the array emits a high quality beam with a single lobe in the far field and power proportional to N^2. Achievement of in-phase synchronization of the individual emitters in a laser array is, however, a complicated task, which usually requires the presence of global coupling between the emitters (see e.g. [14, 15, 25]). An alternative approach which utilizes anti-phase synchronization of adjacent stripes in the array by means of an off-axis feedback from an external cavity was used in [3, 7, 9, 11, 12, 16, 22, 29]. By a proper tilt of the feedback mirror a single transverse supermode of the array characterized by a two-lobe far field pattern can be selected. One of these lobes is reflected back from the feedback mirror and, hence, provides a feedback mechanism necessary for laser generation, while the other one is used for output of laser radiation.

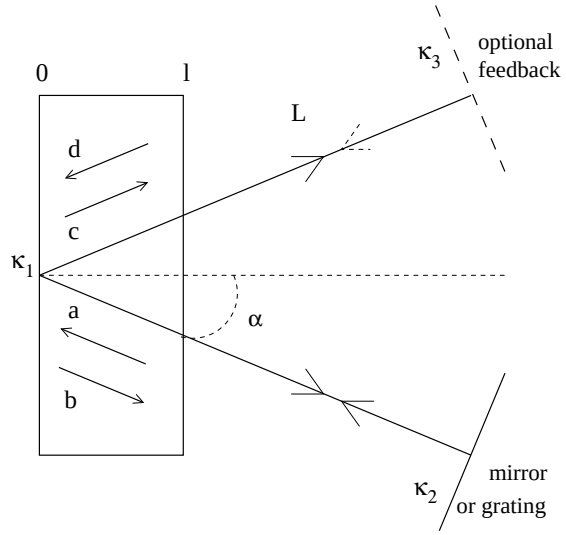

Figure 1: Schematic view of a BAL with off-axis feedback.

In the present work we perform a detailed theoretical investigation of the operation regimes in a multistripe semiconductor laser array with off-axis filtered feedback [18] and extend our analysis to the case of a broad area laser (BAL) with external V-shaped cavity. In Section 2 we introduce mathematical models to study the dynamics of a multistripe laser with a single and two tilted feedback mirrors, which are based on a set of delay differential equations for the electric field envelopes, homogeneous component of the carrier density, and the transverse carrier grating. Section 3 is devoted to numerical analysis of the model equations. For a laser array with a single feedback mirror the bifurcation analysis shows the existence of single and multimode instabilities leading to a periodic and irregular time dependence of the output intensity. In the case of two feedback mirrors we report the formation of a periodic pattern resulting from the interference of the two plane waves reflected from the feedback mirrors. Concluding remarks are given in Section 4.

2 Reduced models of striped BAL with off-axis feedback

Schematic representation of the striped BAL under consideration is shown in Fig. 1. Here, κ_1, κ_2, and κ_3 describe the reflectivity of the left laser facet, feedback mirror, and optional second feedback mirror, respectively; α is the angle of the tilt of the feedback mirror and L is the distance from the right laser facet to this mirror. The distance L is assumed to be much larger than the width w and the length l of the BAL, $L \gg w, l$. The time required for the light to travel from the BAL to the feedback mirror and back is given by $\tau = 2L/c_0$, where c_0 is the velocity of light in vacuum.

When the tilt angle α of the external mirror is properly adjusted, so that the adjacent stripes are syncronized anti-phase, the array emits a double lobed far field pattern with a pronounced output lobe at the angle α and a slightly suppressed feedback lobe at the opposite angle $-\alpha$.

This behavior was observed experimentally [10] and reproduced in numerical simulations using a 2+1 dimensional traveling wave model [18]. Based on this observation we assume that the amplitude of the electric field in the laser cavity can be written as a superposition of four traveling waves with slowly varying envelopes $a(t,z)$, $b(t,z)$, $c(t,z)$, and $d(t,z)$, see Fig. 1,

$$E = ae^{ikz+i\beta x} + ce^{-ikz+i\beta x} + be^{-ikz-i\beta x} + de^{ikz-i\beta x}. \tag{1}$$

Here k is the longitudinal wavevector and the transverse wavevector β is proportional to $\sin\alpha$.

The equation for the carrier density $n(t,z,x)$ can be written in the form

$$\partial_t n = N(x) - \gamma n - n|E|^2, \tag{2}$$

where $N(x) \geq 0$ describes the transverse distribution of the pump current in the semiconductor medium, γ is the carrier relaxation rate and the electric field amplitude E is defined by Eq. (1). Substituting $n = n_0 + n_2 e^{-2i\beta x} + n_2^* e^{2i\beta x} + ...$ into the carrier equation (2) and neglecting fast oscillating terms by assuming that the corresponding coefficients decrease with increasing β ($|n_2| \ll |n_0|$), we obtain the following equations for the homogeneous component of the carrier density n_0 and transverse carrier grating n_2:

$$\begin{aligned}\partial_t n_0 = N_0 - \gamma n_0 - \big(&n_0(|a|^2+|b|^2+|c|^2+|d|^2)+\\ &n_2 cb^* + n_2^* c^* b + n_2 ad^* + n_2^* a^* d\big),\end{aligned} \tag{3}$$

$$\partial_t n_2 = N_2 - \gamma n_2 - \left(n_2(|a|^2+|b|^2+|c|^2+|d|^2) + n_0 c^* b + n_0 a^* d\right), \tag{4}$$

where $N_0 = \int_0^w N(x)dx$ and $N_2 = \int_0^w N(x)e^{2i\beta x}dx$.

For the space-time evolution of the amplitudes a, b, c, and d we write the following system of equations

$$\partial_t a - v_0\partial_z a = \frac{g(1-i\alpha_H)}{2}\left(n_0 a + n_2^* d\right), \tag{5}$$

$$\partial_t d - v_0\partial_z d = \frac{g(1-i\alpha_H)}{2}\left(n_0 d + n_2 a\right), \tag{6}$$

$$\partial_t c + v_0\partial_z c = \frac{g(1-i\alpha_H)}{2}\left(n_0 c + n_2^* b\right), \tag{7}$$

$$\partial_t b + v_0\partial_z b = \frac{g(1-i\alpha_H)}{2}\left(n_0 b + n_2 c\right), \tag{8}$$

where α_H is the linewidth enhancement factor, g is the differential gain parameter, and v_0 is the group velocity of light in semiconductor medium.

The boundary conditions for the laser with a single and two external feedback mirrors are given by

$$\begin{aligned}d(t,l) = 0, \quad b(t,0) = \kappa_1 d(t,0), \quad c(t,0) = \kappa_1 a(t,0),\\ a(t,l) = \kappa_2\Gamma\int_0^t e^{-\Gamma(t-s)} b(s - \frac{2L}{c_0}, l)ds,\end{aligned} \tag{9}$$

and

$$
\begin{aligned}
d(t,l) &= \kappa_3\Gamma\int_0^t e^{-\Gamma(t-s)}c(s-\frac{2L}{c_0},l)ds, \quad b(t,0)=\kappa_1 d(t,0),\\
a(t,l) &= \kappa_2\Gamma\int_0^t e^{-\Gamma(t-s)}b(s-\frac{2L}{c_0},l)ds, \quad c(t,0)=\kappa_1 a(t,0),
\end{aligned}
\tag{10}
$$

respectively. Here we have assumed that Lorentzian spectral filters with the bandwidth Γ are located at the external mirrors.

In the following analysis we assume that the variables n_0, n_2, and E are slowly varying functions of time t inside the active medium ($l \ll L$). Therefore, using an approach similar to that proposed in [23, 26, 27] we can reduce the model equations (3)-(8) to a set of delay differential equations (DDE). In the case of BAL with a single feedback mirror we integrate equations (5)-(8) along the characteristics and use the boundary conditions (9). Then, assuming that $\arg n_2(t,z)$ changes very slowly within the active medium, we obtain the following reduced DDE model for a laser array with a single feedback mirror (see Appendix):

$$\Gamma^{-1}\partial_t A + A = (1-i\alpha_H)\kappa_1\kappa_2 e^{(1-i\alpha_H)G_T}H_T A_T, \tag{11}$$

$$\partial_t G = G_0 - \gamma G - |A|^2(e^G-1)(1+\kappa_1^2 e^G). \tag{12}$$

$$
\begin{aligned}
\partial_t H = H_0 - \gamma H - |A|^2 H\Bigg(&\frac{1-i\alpha_H}{2}e^G(\kappa_1^2(2e^G-1)+1)+\\
&\frac{1+i\alpha_H}{2}\frac{e^G-1}{G}(\kappa_1^2 e^G+1)\Bigg),
\end{aligned}
\tag{13}
$$

where $A(t)=a(t,l)$, $\phi(t)=\arg n_2(t-l/(2v_0),l/2)$, $G(t)=\int_0^l n_0(t-l/(2v_0),z)d\zeta$, $|H(t)|=\int_0^l |n_2(t-l/(2v_0),z)|dz$, and $H(t)=e^{i\phi(t)}|H(t)|$. The subscript T denotes delayed argument, $\phi_T=\phi(t-T)$, $H_T=H(t-T)$, and $G_T=G(t-T)$. The delay time is $T=2(L/c_0+l/v_0)$. In the derivation of (11)-(13) we have used approximations $|n_2| \ll 1$ and $|A| \ll 1$, which are valid when the array operates sufficiently close to the lasing threshold and/or the transverse grating in the active medium is sufficiently weak, see Appendix and Ref. [20]. It will be shown below that despite the above mentioned approximations, the results obtained with our DDE models are in a good qualitative agreement with those of numerical simulations with the 2+1 dimensional traveling wave model [18].

In the case of a BAL with V-shaped external cavity we use a similar procedure and the boundary conditions (10) to obtain the following DDE model

$$\Gamma^{-1}\partial_t A + A = \kappa_2\kappa_1 e^{(1-i\alpha_H)G_T}((1-i\alpha_H)H_T A_T + D_T), \tag{14}$$

$$\Gamma^{-1}\partial_t D + D = \kappa_3\kappa_1 e^{(1-i\alpha_H)G_T}((1+i\alpha_H)H_T^* D_T + A_T), \tag{15}$$

$$\partial_t G = G_0 - \gamma G - (|A|^2+|D|^2)(e^G-1)(1+\kappa_1^2 e^G), \tag{16}$$

$$\partial_t H = H_0 - DA^*(e^G-1)(\kappa_1^2 e^G+1) - \gamma H. \tag{17}$$

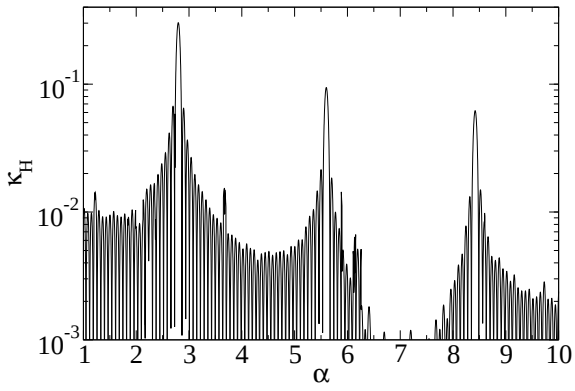

Figure 2: Dependence of the ratio $\kappa_H = |H_0|/G_0$ on the tilt angle α. The main peaks are located at $\alpha \approx 2.8, 5.6, 8.4$ degrees.

where $A(t) = a(t, l)$ and $D = d(t, l)$. In our numerical simulations we have used the following values of the parameters of Eqs. (11)-(13) and Eqs. (14)-(17),

$$T = 2.5,\ \gamma = 0.065,\ \Gamma = 2/T,\ \kappa_1 = 0.95,\ \kappa_2 = 0.9,$$

which are in agreement with those used in the simulations of the 2+1 dimensional traveling wave model in [18].

The parameters H_0 and G_0 in the model equations (11)-(13) and (14)-(17) act as pump parameters for the homogeneous component of the carrier density G and the carrier grating H, respectively. They are proportional to the laser injection current: $G_0 = lN_0 = l\int_0^w N(x)dx$ and $H_0 = lN_2 = l\int_0^w N(x)e^{2i\beta x}dx$. Therefore, the ratio $H_0/G_0 = \kappa_H e^{i\phi_H}$, where $\kappa_H \leq 1$ and ϕ_H are real amplitude and phase, respectively, must be independent of this current. On the other hand, as it is seen from Fig. 2, due to the strong dependence of H_0 on the mirror tilt angle α the quantity κ_H also depends strongly on α. The data shown in this figure were calculated assuming a stepwise dependence of the carrier density on the transverse coordinate x in the array, i.e., $N(x) = 1$ inside the stripes ($x \in [jd_s, jd_s + w_s]$) and $N(x) = 0$ between the stripes ($x \in [jd_s + w_s, (j + 1)d_s]$), where d_s, w_s, and j is the transverse period of the array, stripe width, and stripe number respectively. The value of H_0 was evaluated with $\beta = 2\pi \sin\alpha/\lambda_0$ using the parameters of the real device [10], array width $w = 400$ μm, array period $d_s = 10$ μm, stripe width $w_s = 4$ μm, and wavelength of light $\lambda_0 = 976$ nm. It is seen from Fig. 2 that the quantity κ_H reaches its maximums at the resonant angles $\alpha \approx j\lambda_0/2d_s$ ($\kappa_H \approx 0.8$ for $j = 1$). However, small changes in the tilt angle from a resonant value can lead to a significant decrease of κ_H down to 10^{-3}.

3 Numerical results

Numerical analysis of the model equations (11)-(13) and (14)-(17) has been performed using the routines for direct numerical integration of the delay differential equations and the software package DDE-Biftool [4] for bifurcation analysis of delay differential equations.

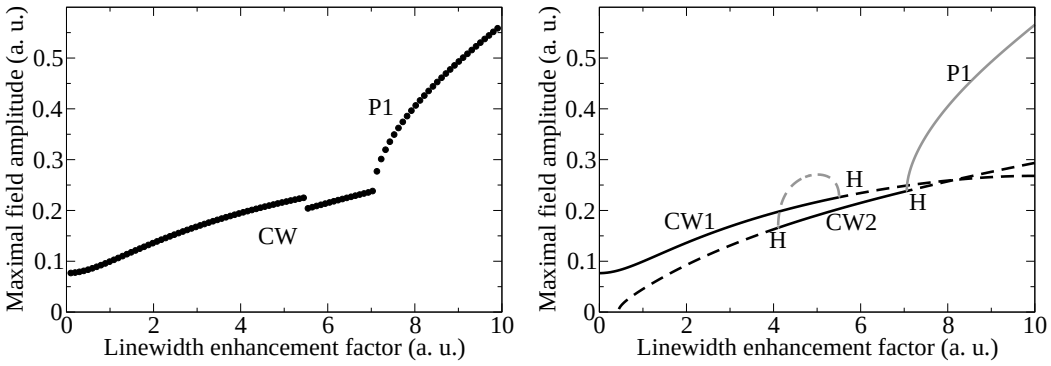

(a) Numerical integration (b) DDE-biftool

Figure 3: Bifurcation tree obtained by numerical integration of the model equations (11)-(13) (a) and with help of DDE-biftool software package (b). Linewidth enhancement factor α acts as a bifurcation parameter. Solid black line: stable CW solution. Dashed black line: unstable CW solution. Solid gray line: stable periodic solution. Solid dashed line: unstable periodic solution. H indicates an Andronov-Hopf bifurcation point. Other parameter values are: $T = 2.5, \gamma = 0.065$, $\Gamma = 2/T$, $\kappa_1 = 0.95$, $\kappa_2 = 0.9$, $G_0 = 0.07$, and $\kappa_H = 0.8$.

3.1 Striped BAL with a single off-axis feedback

In this Section we perform numerical analysis of Eqs. (11)-(13) obtained for the case of external cavity formed by a single feedback mirror. For zero linewidth enhancement factor, $\alpha_H = 0$, we observe only CW regimes with time independent output intensity. On the other hand, when $\alpha_H > 0$, more complicated dynamical regimes can develop in the laser. First, we fix $G_0 = 0.07$ and $\kappa_H = 0.8$, and use the linewidth enhancement factor α_H as a bifurcation parameter. Fig. 3(a) shows the maxima of the time trace of the field amplitude $|A(t)|$ vs parameter α_H within the interval $\alpha_H \in (0, 10)$. It is seen that the field amplitude increases with the parameter α_H. This result can be understood by noticing, that in addition to carrier grating a refractive index grating is created in the semiconductor medium due to the presence of the linewidth enhancement factor. Both these gratings enhance the coupling between the counter-propagating waves a and b (c and d), see Fig. 1, and, hence, lead to a decrease of the cavity losses. Formally the increase of the field amplitude with α_H is related to the presence of the factor $1 - i\alpha_H$ in the right hand side of Eq. (11). A CW regime looses stability at $\alpha_H \approx 7$ via an Andronov-Hopf bifurcation H giving birth to a solution P1 with periodically oscillating laser intensity. The oscillation period is approximately 4 times larger than the external cavity round trip time T, see Fig. 4(a). Therefore, these oscillations appearing due to the presence of transverse grating in the semiconductor medium involve only a single longitudinal mode of the external cavity.

Figure 3(b) shows two branches of CW regimes, $CW1$ and $CW2$, corresponding to two different longitudinal modes of the BAL with external feedback. These branches were calculated using the software package DDE-biftool. With the increase of α_H the solution $CW1$ looses and the solution $CW2$ gains stability via subcritical Andronov-Hopf bifurcations giving rise to a branch of unstable periodic solutions. Bistability between the two CW solutions is observed within a certain range inside the interval $\alpha_H \in (4, 6)$. At $\alpha_H \approx 7$ the solution $CW2$ becomes unstable again via a supercritical Andronov-Hopf bifurcation leading to the appearance of stable

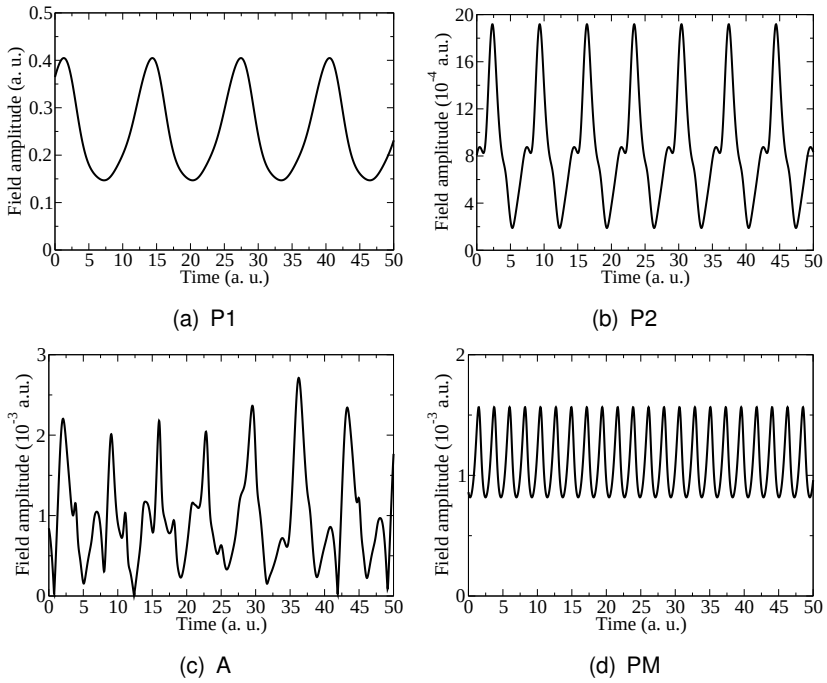

Figure 4: Field amplitude time traces for different regimes. P1: periodic regime with one peak, $G_0 = 0.07$, $\kappa_H = 0.8$, and $\alpha_H = 8$. P2: periodic regime with two peaks, $G_0 = 1$, $\kappa_H = 0.001$, and $\alpha_H = 2.2$. A: aperiodic regime, $G_0 = 1$, $\kappa_H = 0.001$, and $\alpha_H = 3.2$. PM: multimode periodic regime, $G_0 = 1$, $\kappa_H = 0.001$, and $\alpha_H = 4.6$. Other parameter values are as in Fig. 3.

periodic solution $P1$, see Fig 4(b).

At $G_0 = 1$ and $H_0 = 0.001$ the dynamical behavior of the system is even more complicated, see Fig. 5(a). When the α_H factor is increased, CW regimes start to alternate with the pulsed ones labeled by P2 in Fig. 4(b). The periods of these regimes are close to $2T$. With further increase of the parameter α_H periodic pulsations are transformed into aperiodic ones (A), see Fig. 4(c), but still remain single mode. Multimode pulsations PM with the period close to T appear only at $\alpha_H \approx 4.6$, see Fig. 4(d). A bifurcation diagram obtained using the software package DDE-biftool is presented in Fig. 5(b). It is seen that, when the parameter α_H is increased, CW solutions corresponding to different longitudinal modes gain and lose stability via Andronov-Hopf bifurcations. Similarly to the diagram shown in Fig. 3(b) at sufficiently small α_H all these bifurcations are subcritical giving rise to unstable periodic solutions connecting different CW branches. When the linewidth enhancement factor is further increased supercritical Andronov-Hopf bifurcations appear, leading to branches of stable periodic solutions. As it is seen from Fig. 3(b), these periodic branches can have one or more stable parts limited by different bifurcations: Andronov-Hopf bifurcation H, limit cycle fold bifurcation U, torus bifurcation T, and period doubling bifurcation P.

High-power CW operation in BALs is attractive from application point of view. Therefore, it is instructive to look at the stability domains of CW regimes in the plane of two parameters, the linewidth enhancement factor α_H and the pump parameter G_0. According to Figs. 3 and 5, for

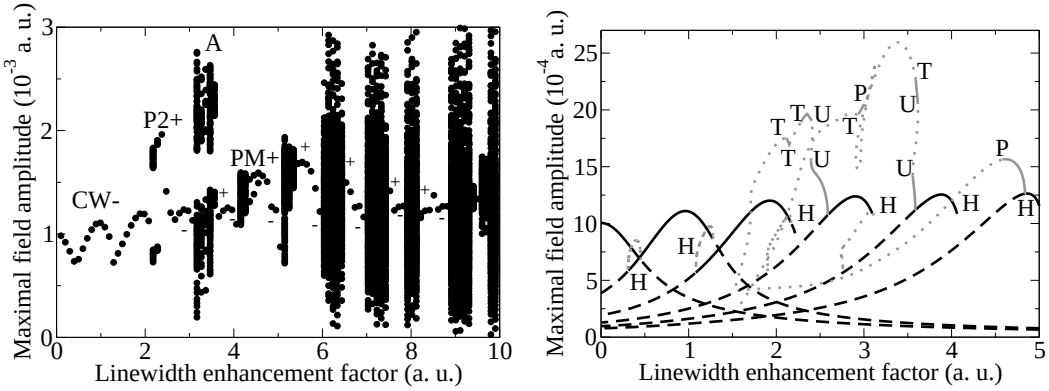

(a) (b)

Figure 5: Bifurcation diagrams obtained by direct numerical integration of Eqs. (11)-(13) (a) and with the help of the software package DDE-biftool. $G_0 = 1$, and $\kappa_H = 0.001$. Notations are the same as in Fig. 3. U: fold bifurcation of a limit cycle. T: torus bifurcation. P: period-doubling bifurcation. Other parameter values are as in Fig. 3.

smaller $\kappa_H = |H_0|/G_0$ the instability of CW states appears at lower values of the linewidth enhancement factor α_H. This is in agreement with the diagram in Fig. 6(a), where the domains of stable CW operation obtained by direct numerical integration of (11)-(13) are shown for two different values of parameter κ_H, $\kappa_H = 0.8$ (solid line) and $\kappa_H = 0.1$ (dashed line). We see that for almost all values of the pump parameter G_0 the instability of a CW solution corresponds to smaller values of the linewidth enhancement factor at $\kappa_H = 0.1$ than at $\kappa_H = 0.8$. This suggests that at moderate values of α_H the stability domains of CW regimes can be enlarged by a proper adjustment of the mirror tilt angle α. For $\kappa_H = 0.1$ instead of a single stability domain we observe three disconnected stability domains of CW solutions corresponding to different longitudinal modes of the external cavity formed by the feedback mirror and carrier grating in the laser medium, see Fig. 6(a). Figure 7 presents a diagram similar to that shown in Fig. 6(a), but corresponds to a larger interval of pump parameters G_0. In this figure different values of the CW field amplitude are shown by different levels of gray color. For $\kappa_H = 0.1$ the first and second stability domains persist for high values of $G_0 \leq 20$, whereas the third domain exists only for $G_0 < 5$, see Fig. 7(b). It follows from the figure that the maximal values of the the laser output power can be achieved at moderate values of the linewidth enhancement factor close to the instability boundary of the CW regime.

3.2 BAL with two feedbacks

Let us consider the case of a BAL with two feedback mirrors forming a V-shaped external cavity (see Fig. 1). In this case the transverse carrier grating n_2 is induced by interference of two waves with opposite transverse wavenumbers reflected from the feedback mirrors and, therefore, the laser generation is possible even with the pump distributed homogeneously in the lateral direction ($H_0 = 0$ in Eqs. (14)-(17)). Similarly to a bidirectional laser and a laser operating in several transverse modes, see e.g. [24], [1], this carrier grating can be responsible for the destabilization of CW states and appearance of non-stationary regimes of operation.

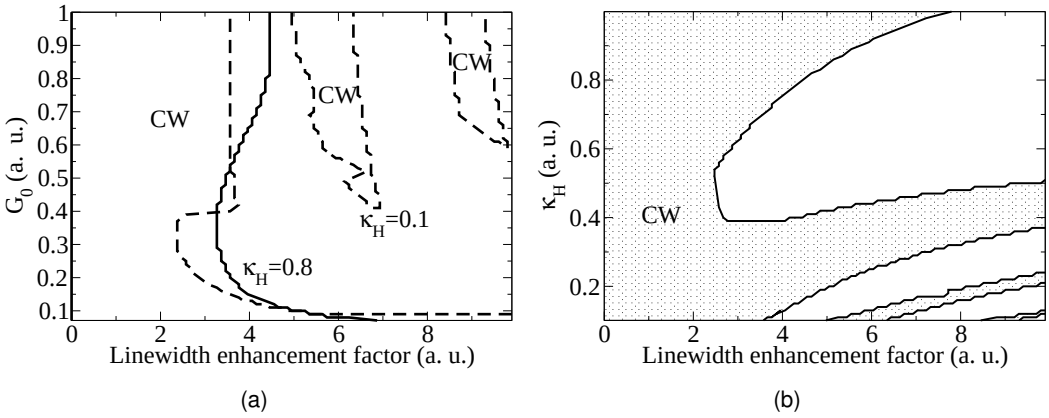

Figure 6: Stability domains of CW regimes in the plane of two parameters: (a) G_0 and α_H, $\kappa_H = 0.1$ (dashed), $\kappa_H = 0.8$ (solid); (b) κ_H and α_H, $G_0 = 1$. Other parameter values are as in Fig.3.

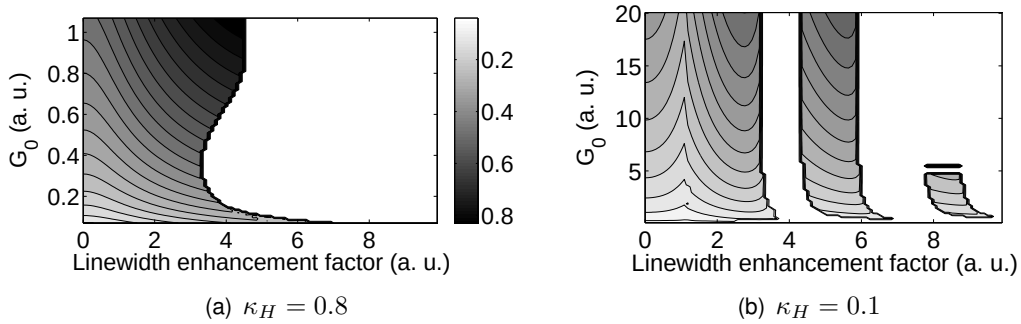

Figure 7: Stability domains of CW regimes with different field amplitudes $|E|$ on the plane of two parameters, α_H and G_0. (a) – $\kappa_H = 0.1$ and (b) – $\kappa_H = 0.8$. The highest value of the amplitude $|E|$ corresponds to the black color. Other parameters are as in Fig.3.

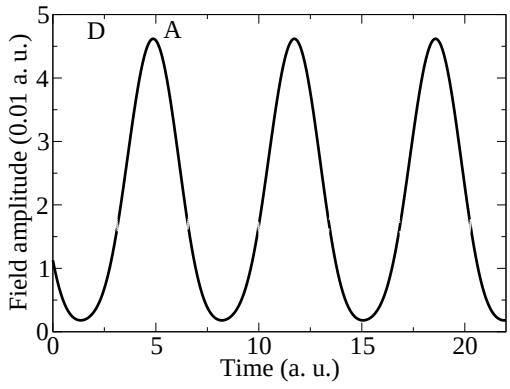

Figure 8: Periodic antiphase pulsations of the output field amplitudes $|A|$ and $|D|$ in a BAL with two feedback mirrors. $G_0 = 0.07$, $H_0 = 0$, $\alpha_H = 0.1$, $T = 2.5$, $\gamma = 0.065$, $\Gamma = 2/T$.

In particular, it was shown in Ref. [18], using a 2+1 dimensional traveling wave model, that a homogeneously pumped BAL with two feedback mirrors can exhibit a regime characterized by $2T$-periodic anti-phase pulsations of the amplitudes of two counter-propagating waves, $|A(t)|$ and $|D(t)|$. This regime assumes the generation of more than one longitudinal mode of the external cavity. A similar anti-phase multi-mode regime obtained by numerical integration of the DDE model (14)-(17) is presented in Fig. 8, which demonstrates good agreement with the results reported in [18].

4 Conclusion

We have studied the dynamics of broad area lasers with a single tilted feedback mirror and a V-shaped external cavity formed by two off-axis feedback mirrors. Starting from traveling wave equations we have derived reduced DDE models for the amplitudes of the plane waves propagating in the cavity, transversely homogeneous component of the carrier density, and transverse carrier grating in the semiconductor medium. Bifurcation analysis of the reduced model indicates that at sufficiently large values of the injection current and the linewidth enhancement factor different instabilities of CW regimes can develop in the system. In particular, an Andronov-Hopf bifurcations are responsible for the destabilization of CW regimes and appearance of single mode and multimode pulsations. Periodic anti-phase pulsation of the output intensities of several longitudinal modes of the external cavity observed earlier in numerical simulations of the traveling wave model [18] are well reproduced with the help of the reduced model. Finally, parameter scans show that the stability domain of CW operation in a multistripe laser array with a single feedback mirror can be enlarged by proper adjustment of the tilt angle of this mirror.

5 Appendix

Here we describe shortly the derivation of (11)-(13). We suppose that $\arg n_2(t,z)$ varies slowly in t and z. Then integrating Eqs. (5)-(8) along the characteristics we obtain from the following approximate relations between the field amplitudes at the left ($z=0$) and right ($z=l$) laser facets:

$$a(t,0) \approx e^{G_\alpha^-}\left[a(t-l/v_0,l)\cosh H_\alpha^- + e^{-i\phi}d(t-l/v_0,0)\sinh H_\alpha^-\right], \tag{18}$$

$$d(t,0) \approx e^{G_\alpha^-}\left[d(t-l/v_0,l)\cosh H_\alpha^- + e^{i\phi}a(t-l/v_0,l)\sinh H_\alpha^-\right], \tag{19}$$

$$b(t,l) \approx e^{G_\alpha^+}\left[b(t-l/v_0,0)\cosh H_\alpha^+ + e^{i\phi}c(t-l/v_0,0)\sinh H_\alpha^+\right], \tag{20}$$

$$c(t,l) \approx e^{G_\alpha^+}\left[c(t-l/v_0,0)\cosh H_\alpha^+ + e^{-i\phi}b(t-l/v_0,0)\sinh H_\alpha^+\right], \tag{21}$$

where $G^+(t) = \int_0^l n_0(t - z/v_0, z)dz$, $G^-(t) = \int_0^l n_0(t - (l-z)/v_0, z)dz$, $H^+(t) = \int_0^l |n_2(t-z/v_0,z)|dz$, $H^-(t) = \int_0^l |n_2(t-(l-z)/v_0,z)|d\zeta$, and the subscript α indicates that the term is multiplied by $(1-i\alpha_H)/2$.

By differentiating the last relation in the boundary conditions (9) we obtain

$$\Gamma^{-1}\partial_\tau a(t,l) + a(t,l) = \kappa_2 b(t - 2L/c_0, l).$$

Using Eqs. (18)-(21) and boundary conditions Eqs. (9) we can write the following equation for $A(t) \equiv a(t,l)$

$$\Gamma^{-1}\partial_t A + A = \kappa_1\kappa_2 e^{\frac{1-i\alpha}{2}(G_T^+ + G_T^-)} e^{i\phi_T} A_T \times \Big\{ \sinh\frac{1-i\alpha}{2} H_T^- \cosh\frac{1-i\alpha}{2} H_T^+ + \cosh\frac{1-i\alpha}{2} H_T^- \sinh\frac{1-i\alpha}{2} H_T^+ \Big\}, \tag{22}$$

where $\phi_T = \phi(t-T)$, $H_T^\pm = H^\pm(t-T)$, $G_T^\pm = G^\pm(t-T)$, and $T = 2(L/c_0 + l/v_0)$.

Assuming that the the variables n_0, n_2, and A are slowly varying functions of t and using the fact that the active medium length is much smaller than the external cavity length, $l \ll L$, we get the following relations:

$$G^+ \approx G^- \approx G, \qquad H^+ \approx H^- \approx |H|.$$

Substituting these relations into (22) and assuming that the absolute value of n_2 is small we obtain Eq. (11). The equation (12) for the variable G is derived by integrating Eq. (3) over the active medium length l and using (18)-(21) together with the approximate relations $H(t - l/v_0) \approx H(t)$ and $G(t - l/v_0) \approx G(t)$. The equation (13) for $H = |H|e^{i\phi}$ is obtained in a similar way by integrating Eq. (4) with additional approximation $|A| \ll 1$. More details on the derivation of Eqs. (11)-(13) and Eqs. (14)-(17) can be found in [20].

References

[1] I. Babushkin, U. Bandelow, and A. G. Vladimirov. Rotational symmetry breaking in small-area circular vertical cavity surface emitting lasers. *Opt. Commun.*, 284:1299–1302, 2011.

[2] D. Botez and D. R. Scifres, editors. *Diode Laser Arrays*. Cambridge University Press, 1994.

[3] M. Chi, B. Thestrup, and P. M. Petersen. Self-injection locking of an extraordinarily wide broad-area diode laser with a 1000-μm-wide emitter. *Opt. Lett.*, 30:1147–1149, 2005.

[4] K. Engelborghs, T. Luzyanina, and G. Samaey. DDE-BIFTOOL v.2.00: A MATLAB package for bifurcation analysis of delay differential equations. Technical Report TW-330, Department of Computer Science, K.U.Leuven, Leuven, Belgium, 2001.

[5] C. Fiebig, G. Blume, C. Kaspari, D. Feise, J. Fricke, M. Matalla, W. John, H. Wenzel, K. Paschke, and G. Erbert. 12W high-brightness single-frequency DBR tapered diode laser. *Electron. Lett.*, 44:1253–1255, 2008.

[6] C. Fiebig, V. Z. Tronciu, M. Lichtner, K. Paschke, and H. Wenzel. Experimental and numerical study of Distributed-Bragg-Reflector tapered lasers. *Appl. Phys. B*, 99:209–214, 2010.

[7] L. Goldberg and J. Weller. Narrow lobe emission of high power broad stripe laser in external resonator cavity. *Electron. Lett.*, 25:112–114, 1989.

[8] K.-H. Hasler, B. Sumpf, P. Adamiec, F. Bugge, J. Fricke, P. Ressel, H. Wenzel, G. Erbert, and G. Trankle. 5-W DBR tapered lasers emitting at 1060 nm with a narrow spectral linewidth and a nearly diffraction-limited beam quality. *IEEE Phot. Techn. Lett.*, 20:1648–1650, 2008.

[9] K. Iida, H. Horiuchi, O. Matoba, T. Omatsu, T. Shimura, and K. Kuroda. Injection locking of a broad-area diode laser through a double phase-conjugate mirror. *Opt. Commun.*, 146:6–10, 1998.

[10] A. Jechow, M. Lichtner, R. Menzel, M. Radziunas, D. Skoczowsky, and A. G. Vladimirov. Stripe-array diode-laser in an off-axis external cavity: theory and experiment. *Opt. Express*, 17:19599–19604, 2009.

[11] A. Jechow, V. Raab, and R. Menzel. Tunable 6.8 W narrow bandwidth emission from a single-stripe continuous-wave broad-area laser diode in a simple external cavity. *Appl. Opt.*, 47:1447–1450, 2008.

[12] A. Jechow, V. Raab, R. Menzel, M. Cenkier, S. Stry, and J. Sacher. 1 W tunable near diffraction limited light from a broad area laser diode in an external cavity with a line width of 1.7 MHz. *Opt. Commun.*, 277:161–165, 2007.

[13] M. Kanskar, T. Earles, T.J. Goodnough, E. Stiers, D. Botez, and L. J. Mawst. 73% CW power conversion efficiency at 50 W from 970 nm diode laser bars. *Electron. Lett.*, 41:245–247, 2005.

[14] G. Kozyreff, A. G. Vladimirov, and P. Mandel. Global coupling with time delay in an array of semiconductor lasers. *Phys. Rev. Lett.*, 85(18):3809–3812, 2000.

[15] G. Kozyreff, A. G. Vladimirov, and P. Mandel. Dynamics of a semiconductor laser array with delayed global coupling. *Phys. Rev. E*, 64(1):16613 (12 pages), 2001.

[16] L. Lang, J. J. Lim, S. Sujecki, and E. C. Larkins. Improvement of the beam quality of a broad-area diode laser using asymmetric feedback from an external cavity. *Opt. Quantum. Electron.*, 40:1097–1102, 2008.

[17] H. Li, I. Chyr, X. Jin, F. Reinhardt, T. Towe, D. Brown, T. Nguyen, M. Berube, T. Truchan, D. Hu, R. Miller, R. Srinivasan, T. Crum, E. Wolak, R. Bullock, J. Mott, and J. Harrison. $>$700W continuous-wave output power from single laser diode bar. *Electron. Lett.*, 43:27–28, 2007.

[18] M. Lichtner, V. Z. Tronciu, and A. G. Vladimirov. Theoretical investigation of striped and non-striped broad area lasers with off-axis feedback. *IEEE*, 48:353–360, 2012.

[19] K. J. Paschke, S. Einfeldt, A. Ginolas, K. Haeusler, P. Ressel, B. Sumpf, H. Wenzel, and G. Erbert. 15 -W reliable operation of 96 -μm aperture broad-area diode lasers emitting at 980 nm. In *CLEO/QELS Conference and Photonic Applications Systems Technologies*, OSA Technical Digest (CD), paper CMN4, 2008.

[20] A. Pimenov, G. Kozyreff, V. Z. Tronciu, and A. G. Vladimirov. Theoretical analysis of a multi-stripe laser array with external off-axis feedback. In Krassimir Panajotov, editor, *Semiconductor Lasers and Laser Dynamics V*, volume 8432 of *Proc. SPIE*, page 0, 2012.

[21] M. Spreemann, M. Lichtner, M. Radziunas, U. Bandelow, and H. Wenzel. Measurement and simulation of distributed-feedback tapered master-oscillator power amplifiers. *IEEE J. Quantum Electron.*, 45:609–616, 2009.

[22] B. Thestrup, M. Chi, and P. M. Petersen. Lateral mode selection in a broad-area laser diode by self-injection locking with a mirror stripe. In Mark S. Zediker, editor, *High-Power Diode Laser Technology and Applications*, volume 5336 of *Proc. SPIE*, page 38, 2004.

[23] A. G. Vladimirov, D. Turaev, and G. Kozyreff. Delay differential equations for mode-locked semiconductor lasers. *Opt. Lett.*, 29:1221–1223, 2004.

[24] A.G. Vladimirov. Bifurcation analysis of a bidirectional class B laser. *Optics Communications*, 149(1-3):67–72, 1998.

[25] A.G. Vladimirov, G. Kozyreff, and P. Mandel. Synchronization of weakly stable oscillators and semiconductor laser arrays. *Europhysics Letters*, 61(5):613 –619, 2003.

[26] A.G. Vladimirov and D. Turaev. New model for mode-locking in semiconductor lasers. *Radiophys. & Quant. Electron.*, 47(10-11):857–865, 2004.

[27] A.G. Vladimirov and D. Turaev. Model for passive mode-locking in semiconductor lasers. *Phys. Rev. A*, 72:033808 (13 pages), 2005.

[28] H. Wenzel, K. Paschke, O. Brox, F. Bugge, J. Fricke, A. Ginolas, A. Knauer, P. Ressel, and G. Erbert. 10W continuous-wave monolithically integrated master-oscillator power-amplifier. *Electron. Lett.*, 43:160–161, 2007.

[29] S. Wolff, A. Rodionov, V. Sherstobitov, and H. Fouckhardt. Fourier-optical transverse mode selection in external-cavity broad-area lasers: experimental and numerical results. *IEEE J. Quantum Electron.*, 39:448–458, 2003.